

UNDULATED CYLINDER ARRAY DISTRIBUTION EFFECT ON FLOW STRUCTURE DYNAMICS

Ondřej Ferčák,

Department of Mechanical & Materials Engineering
Portland State University
1930 SW 4th Ave # 500, Portland, OR 97201, USA
ofercak@pdx.edu

Zein Sadek

Department of Mechanical & Materials Engineering
Portland State University
1930 SW 4th Ave # 500, Portland, OR 97201, USA
sadek@pdx.edu

Trevor K. Dunt

Department of Engineering Physics
University of Wisconsin–Madison
Madison, WI, USA
dunt@wisc.edu

Christin T. Murphy

Naval Undersea Warfare Center
Newport, RI, USA
christin.t.murphy.civ@us.navy.mil

Jennifer A. Franck

Department of Engineering Physics
University of Wisconsin–Madison
Madison, WI, USA
jafranck@wisc.edu

Raúl Bayoán Cal

Department of Mechanical & Materials Engineering
Portland State University
1930 SW 4th Ave # 500, Portland, OR 97201, USA
rcal@pdx.edu

ABSTRACT

The present study experimentally investigates a bio-inspired (phocid pinniped vibrissae) undulated cylinder (UC) array consisting of nine cylinders at equal spacing in the streamwise (x) and spanwise (y) directions. The UC's longitudinal axes are oriented parallel to the vertical (z) direction. The spatial distributions (x - y) are fixed at three mean UC chord diameters ($3D$) in both the spanwise and streamwise direction. For comparison, a single undulated cylinder and single elliptical cylinder with a mean chord length of the UC are characterized. Particle image velocimetry (PIV) measurements are conducted directly behind the farthest downstream row and used to quantify the momentum and Reynolds stress terms from the Reynolds averaged Navier-Stokes (RANS) equation. The measurements are conducted at five distinct wall normal planes, which span a repeating section of undulations at a Reynolds number of 8,000. The mean spanwise velocities are comparable between the ellipse and array, while the UC exhibits large velocity lobes at the sides of the cylinder. The five separate planes reveal that there is a slightly higher momentum deficit at the trough directly behind the center UC in the array. The vorticity contours show a distinct positive and negative signature in the spanwise direction directly behind each of the two cylinders and each undulated cylinder vorticity is shown to begin interacting at approximately $X/D = 6$. This study provides thorough insight into a valuable bio-inspired engineering model. The results of this study will not only further comparative biological studies, but also provide additional tools for engineers in need of controls schemes or engineering requirements for column structure array designs with reduced wake growth, lift, drag, or vibrations.

INTRODUCTION

Several variations of hydrodynamic, trail-following research has confirmed that pinnipeds (seals) can follow the trail created by prey while blindfolded, which is attributed to the sensitivity and unique geometry of pinniped whiskers (Murphy *et al.* (2013, 2015); Dehnhardt *et al.* (2001); Schulte-Pelkum *et al.* (2007)). The canonical seal whisker geometry resembles an elliptical cylinder with undulations along the elliptical major-axis, which are out of phase with each other and undulations that are in-phase along the minor-axis (Hanke *et al.* (2010)). Experimental work investigating this geometry has also confirmed reduction in vortex induced vibrations, and computational models have been used to further investigate the manipulation of this geometry (Lyons *et al.* (2020)).

For example, a large eddy simulation (LES) study by Hans *et al.* (2013) looked at varying combinations of pinniped-inspired whisker-geometry undulations and found that the reduction in the drag coefficient was dependent on the existence of the undulations on the minor-axis. An extensive LES study regarding this bio-inspired geometry was performed by Lyons *et al.* (2020), who looked at a large geometric parameter space for variations in a pinniped whisker. The result of this study confirmed that the canonical seal whisker geometry outperformed the other geometries with respect to drag, vibration, and vortex reduction. A natural extension of this work is to consider how these hydrodynamic benefits express themselves in an array of such cylinders.

In this study the differences between a single ellipse, a single UC, and an UC array ($3D$ - $3D$ spacing) are experimentally investigated in a wind tunnel. In order to measure the differences in mean flow at different points of interest on the undulated surface, five spanwise-streamwise PIV planes were

recorded. Mean second order statistics were calculated using stereo PIV data. The wake interactions and vorticity are discussed in the following sections.

METHODS

The 3D printed UC array and single geometries were tested in the Portland State University (PSU) wind tunnel. The PSU wind tunnel test section is 0.8 m tall, with a width of 1.2 m and test section length of 5 m as seen in Figure (1). The ceiling of the tunnel was configured to approach a zero-pressure gradient boundary layer. Streamwise-spanwise (x - y) velocity fields are measured using two camera 2D particle image velocimetry (PIV). Four megapixel CCD cameras with 50 mm focal length and a Litron Nano double pulsed Nd:YAG (532 nm, 1200 mJ, 4 ns duration) laser are used to record PIV snapshots. Each array configuration measurement includes 2000 independent image-pairs recorded at 4 Hz and visualized by neutrally buoyant fluid particles of diethyl-hexyl sebacate, aerosolized by a seeding generated holding constant density throughout the experiment.

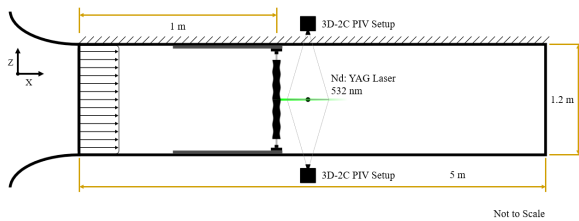


Figure 1. Schematic of Portland State University [PSU] wind tunnel and experimental setup. Single undulated cylinder (UC) visualized at 1 m distance from inlet and stereo PIV plane at center.

The image-pairs are processed with a multipass fast Fourier transform (FFT) based cross-correlation algorithm and universal outlier detection to filter out bad vectors using LaVision DaVis 8.4 imaging software. The PIV data is processed using a multiple pass reducing size interrogation window of 48×48 pixels and 24×24 pixels, and a 50% overlap. The PIV window is $0.2\text{m} \times 0.2\text{m}$ ($6D \times 6D$) in size and its leading edge is $1.5D$ from the center of the farthest UC downstream (Figure 2). Due to the spanwise symmetry of the setup, the PIV window is offset in the positive y -direction (spanwise) so the side edge is $1.5D$ from the center of the middle UC in order to capture as much of the flow as possible. Two planes are recorded for each array configuration spanning a downstream distance of $X/D \in [1.5, 12.5]$ seen in Figure. Farther downstream profiles are significantly recovered past $12.5D$ for the cases in this study. Ensemble averaging is performed over all PIV snapshots to approximate time averaging and outlier removal is employed at 1.5 standard deviations maintaining 80-90% of the original data. The Reynolds numbers, Re_D is 8,000 (3.5 m/s), using the mean chord diameter, D , as the non-dimensional parameter.

The undulated cylinder geometries based on Hanke *et al.* (2010) and Lyons *et al.* (2020) are manufactured for the wind tunnel experiments. The cylinders are scaled up geometrically at a ratio of approximately 1:31 with a mean chord diameter, D , of 33.63 mm and a mean chord thickness, T , of 17.53 mm.

A total of nine identical array UCs are 3D printed on a Stratasys F120 FDM printer with a resolution of ± 0.2 mm

using ABS-M30 black filament. Each UC includes a square opening along the length of the cylinder axis to accommodate a 9.5 mm square steel rod for mounting support and to prevent unwanted vibration. Three separate sections are printed and glued together using an ABS-Acetone slurry to create a total cylinder length of 460 mm. The surface of the cylinder is then wet sanded and sprayed with lacquer to achieve a smooth finish.

An external mould of a UC section is printed with five precision openings to mark longitudinal PIV laser-alignment locations (z -direction), visualized as pink lines seen in Figure 2. The marks are aligned to span the peak-to-peak major-axis undulations on the UC with a calculated spacing of 10.97 mm.

The UC array spacing is simplified by aligning two opposing 4 mm acrylic mounting plates on the top and bottom of the Portland State University (PSU) wind tunnel. The mounting plates include a 22×34 grid of mounting holes laser cut with 1D spacing in both x and y for accurate and efficient array configurations through M3 threaded inserts, which are heat-set into the holes. The UCs are fixed to the mounting plates using a compact 3D printed fixture with an opening and set screw for the steel rod and a base that has corresponding mounting hole locations to the mounting plate.

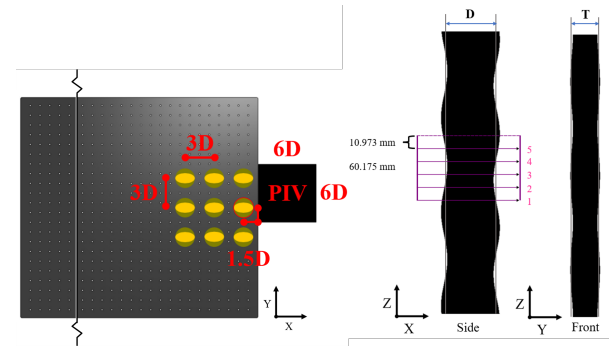


Figure 2. (Left) Undulated cylinder (UC) segment front (right) and side (left) view with diameter, D , of 33.63 mm and thickness, T , of 17.53 mm. Repeating geometry is 60.18 mm and PIV plane markers are spaced at 10.97 mm increments. (right) Top view of mounting plate arrangement of PIV array layout.

RESULTS

In order to characterize the whisker array flow behavior, we first look at the variations between the smooth ellipse, single whisker, and $9 \times$ whisker array. The streamwise velocity, U , for z -plane 3 shown in Figure 3 shows a long and constant narrow wake for the ellipse. The single whisker, in comparison, has a large momentum deficit directly behind the whisker but recovers much more quickly than the ellipse does. The array contour reveals characteristics of both the ellipse and whisker in that a larger deficit is present but recovers faster as the whisker does. However, the overall wake of the array is clearly wider than that of the single whisker.

The spanwise velocity, V , in Figure 3 has dramatic positive and negative side lobes for the whisker in comparison to both the ellipse and array. This is due to the flow divergence caused by the whisker undulations. It is worth noting that the

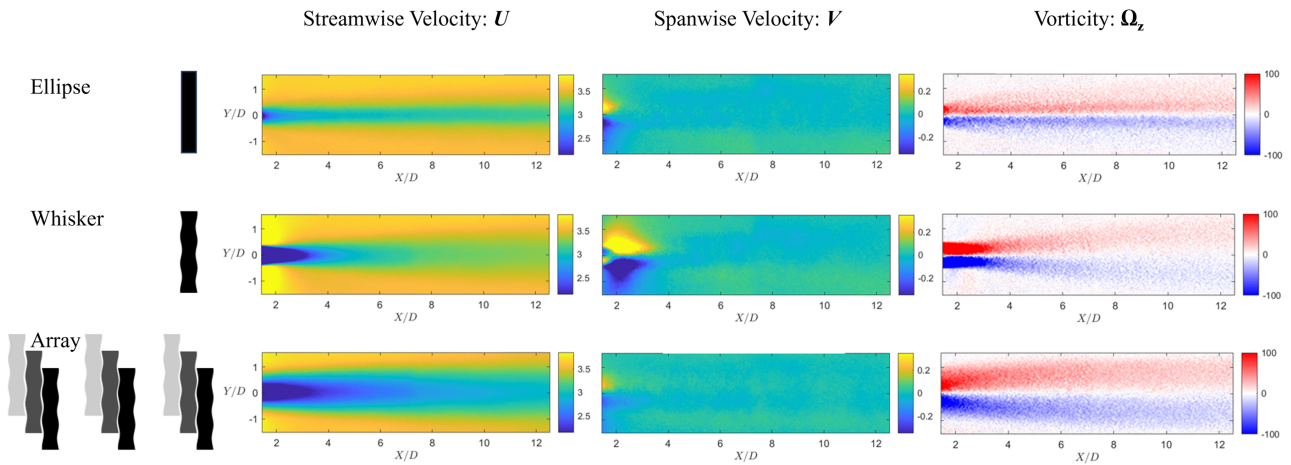


Figure 3. Contours for ellipse, whisker, and array at $Z = 3$, and $U_\infty = 3.5\text{m/s}$: (left) Normalized streamwise velocity, U/U_∞ . (middle) Normalized spanwise velocity, V/U_∞ . (right) Normalized vorticity, $\overline{\Omega_z}(D/U_\infty)$.

array and ellipse have substantially lower spanwise lobes, and that the array even slightly lower.

Figure 3 reveals a similar trend for the vorticity, Ω_z , contours in that the whisker shows a strong signature behind the whisker with a substantial decrease in magnitude downstream. This is in contrast to the relatively constant magnitudes seen in the ellipse and array even though the array width is much wider in the y -direction.

The benefits of a single whisker structure as compared to a smooth cylinder or ellipse are reestablished. Vibration reduction in cylindrical structures, for example, is a common problem. Engineering applications in need of minimal flow disruption are well suited for utilizing this geometry. However, many such application require more than a single column, so an array of structures may come into consideration.

The work described in this manuscript outline the analysis of such structures. It is clear that wake recovery and spanwise velocity are much improved in comparison to even a single smooth column, with the spanwise momentum performing better than even the single whisker. While the vorticity of a single whisker shows large magnitudes directly behind the whisker, the array has a more consistent vorticity signature comparable to one smooth ellipse albeit with a wider wake. Spanwise and streamwise vorticity flux is also minimized for the array indicating that larger coherent structures lose energy within the array itself.

Vorticity transport magnitudes are decreased for the array seen through the inertial and flux terms. This is likely due to the disruption and mixing of the flow throughout the array farm. It should be noted that measurements are at the end of the array which means that some of the differences between single whisker and array likely have incremental behaviour behind each row of the array, which is something future work can investigate.

Applications of this research are far reaching, including bio-inspired sensors to wake recovery in wind-farm arrays (Beem *et al.* (2012a,b); Beem & Triantafyllou (2015)). Large building structures could potentially benefit from the minimization of wind driven forces on the large scale and small scales applications could include structurally sensitive cooling or mixing chambers. Beyond engineering applications, the continued modeling and development of undulated cylinder array research will be critical to future phocid pinniped studies.

REFERENCES

- Beem, Heather, Hildner, Matthew & Triantafyllou, Michael 2012a Calibration and validation of a harbor seal whisker-inspired flow sensor. *Smart Materials and Structures* **22** (1), 014012.
- Beem, Heather, Hildner, Matthew & Triantafyllou, Michael 2012b Characterization of a harbor seal whisker-inspired flow sensor. In *2012 Oceans*, pp. 1–4. IEEE.
- Beem, Heather R & Triantafyllou, Michael S 2015 Wake-induced ‘slaloming’ response explains exquisite sensitivity of seal whisker-like sensors. *Journal of Fluid Mechanics* **783**, 306–322.
- Dehnhardt, Guido, Mauck, Bjorn, Hanke, Wolf & Bleckmann, Horst 2001 Hydrodynamic trail-following in harbor seals (*phoca vitulina*). *Science* **293** (5527), 102–104.
- Hanke, Wolf, Witte, Matthias, Miersch, Lars, Brede, Martin, Oeffner, Johannes, Michael, Mark, Hanke, Frederike, Leder, Alfred & Dehnhardt, Guido 2010 Harbor seal vibrissa morphology suppresses vortex-induced vibrations. *Journal of Experimental Biology* **213** (15), 2665–2672.
- Hans, Hendrik, Miao, Jianmin, Weymouth, Gabriel & Triantafyllou, Michael 2013 Whisker-like geometries and their force reduction properties. In *2013 MTS/IEEE OCEANS-Bergen*, pp. 1–7. IEEE.
- Lyons, Kathleen, Murphy, Christin T & Franck, Jennifer A 2020 Flow over seal whiskers: Importance of geometric features for force and frequency response. *Plos one* **15** (10), e0241142.
- Murphy, Christin T., Eberhardt, William C., Calhoun, Benton H., Mann, Kenneth A. & Mann, David A. 2013 Effect of Angle on Flow-Induced Vibrations of Pinniped Vibrissae. *PLOS ONE* **8** (7).
- Murphy, Christin T, Reichmuth, Colleen & Mann, David 2015 Vibrissal sensitivity in a harbor seal (*phoca vitulina*). *The Journal of Experimental Biology* **218** (15), 2463–2471.
- Schulte-Pelkum, N, Wieskotten, S, Hanke, W, Dehnhardt, G & Mauck, B 2007 Tracking of biogenic hydrodynamic trails in harbour seals (*phoca vitulina*). *Journal of Experimental Biology* **210** (5), 781–787.